Materials Today Nano 3 (2018) 48–53

Contents lists available at ScienceDirect

Materials Today Nano

journal homepage: https://www.evise.com/profile/#/MTNANO/login

Dislocation plasticity reigns in a traditional twinning-induced plasticity steel by *in situ* observation

X. Fu [a], X. Wu [b, c], Q. Yu [a, *]

[a] Center of Electron Microscopy and State Key Laboratory of Silicon Materials, School of Materials Science & Engineering, Zhejiang University, Hangzhou, 310027, China
[b] State Key Laboratory of Nonlinear Mechanics, Institute of Mechanics, Chinese Academy of Sciences, Beijing, 100190, China
[c] School of Engineering Science, University of Chinese Academy of Sciences, Beijing, 100049, China

ARTICLE INFO

Article history:
Available online 14 November 2018

Keywords:
Deformation twinning
Plasticity
Dislocation
TWIP steel
Microstructure

ABSTRACT

To twin or not to twin? The critical doubt emerges recently on the dominant role of deformation twinning in contributing to strain hardening and plasticity, which has been long taken for granted specifically in twinning-induced plasticity (TWIP) steels. Here, the dynamic deformation process was *in situ* studied in a typical Fe-30Mn-3Si-3Al (wt. %) TWIP steel by using transmission electron microscopy. It is found that dislocation activities, instead of twinning, reigns over the whole plastic process, including planar slips and especially cross-slips of dislocations, leading to strong interaction of dislocations. An unexpected generation of nanograins is visible because of dislocation activities ahead of the crack tip. Moreover, the dominant dislocation plasticity continues straight down to cryogenic temperatures. The present results evidence the key role of forest dislocation hardening and shed insights into deformation physics in TWIP steels, contrary to our conventional understanding.

1. Introduction

Twinning-induced plasticity (TWIP) steels have been arousing everlasting concerns, in which plasticity majorly comes from deformation twinning (DT), often called the TWIP effect [1–4]. The general understanding lies in that the twin boundaries (TBs) because of progressively twinning act as obstacles to effectively impede the motion of dislocations and reduce the dislocation mean free path gradually, leading to the dynamic Hall–Petch effect [5–8]. As such, the core of TWIP effect lies in extraordinary strain hardening by DT serving as a key mechanism, while the negligible dislocation forest hardening is often hinted. Hence, a good balanced result between tensile strength and especially superior ductility is obtained. In addition, the alloys of more or less TWIP effect always induce high fracture toughness and fatigue resistant properties [9–12].

Yet, the TWIP effect runs into challenges recently in TWIP steels [13]. Tracing to the TWIP effect, DT contributes to plasticity primarily from the following three aspects [13–17]: (1) the formation of deformation twinning accommodates plastic strain; (2) TBs serve as barriers to dislocation motion; and (3) TBs provide adequate sites for nucleating and accommodating dislocations. In contrast, it is long taken for granted that dislocation behaviors are ignorable, even often observable. This idea gets further intensified especially because of the absence of intragranular cross-slip of dislocations, except for planar slip, in varying TWIP steels with face-centered cubic (fcc) structures of low stacking fault energy (SFE). However, the cross-slip of extended dislocations plays a key effect on work hardening, as the dissolved partials on intersected cross-slip planes may intersect to form Lomer–Cottrell locks, which extraordinarily contributes to work hardening [18]. Actually, DT works through TBs [8,15]. The TBs, if imbedded in grains in advance (e.g. in nanotwinned metals), realize strain hardening by intensifying dislocation-mediated plasticity to produce dislocation generation and strong interplay with TBs. Yet, both the density and spacing of TBs in TWIP steels are usually at least one magnitude lower than that in nanotwinned metals [19,20]. Thereby, the dislocation plasticity may operate freely. Recently, a few results spring up to question whether or not DT indeed plays the dominant role in strain hardening in TWIP steels. For example, it is the forest hardening instead of DT that contributes to up to 90% of flow stress in a Fe-18Mn-0.6C-1.5Al-0.8Si (wt. %) TWIP steel [21]. In a Fe-22Mn-0.6C TWIP steel, DT happens only in part of grains because of orientation anisotropy [14,22]. The quantitative measurement

* Corresponding author.
E-mail address: yu_qian@zju.edu.cn (Q. Yu).

https://doi.org/10.1016/j.mtnano.2018.11.004

reveals a true strain of 0.07 by both DT and martensitic transformation out of total strain of 0.18 in the Fe-22Mn-0.6C pillars [22].

In this article, we made detailed *in situ* observations of dislocation activities to investigate the role of dislocations in strain hardening using a transmission electron microscope (TEM) in a classical Fe-30Mn-3Si-3Al (wt. %) TWIP steel. Specifically, the cross-slip of dislocations and resultant strong interplay of dislocations, along with the generation of nanograins ahead of the crack tip, were observed, which indicates a copious dislocation storage much like that happened in common fcc metals of high SFE. Our results provide solid evidences that dislocation activities, instead of DT, contribute largely to strain hardening in the plastic deformation of TWIP steel.

2. Methods

The as-received material is Fe-30Mn-3Si-3Al TWIP steel, which was heat treated at 950 °C for 1 h to obtain a fully recrystallized microstructure with an average grain size of about 10 μm. The TEM specimens were prepared by mechanical grinding and then thinned by twin-jet electrochemical polishing in a Struers TenuPol-5, using a solution of 95% ethanol and 5% perchloric acid at about −30 °C. *In situ* TEM straining tests were performed at room temperature (RT) and cryogenic temperature, using a Gatan model 671 single-tilt straining holder, in a FEI Tecnai G2 F20 microscope operating at 200 kV. Strain was intermittently applied with a motor at a speed of about 1 μm s^{-1} during each pulse. Atomic structure characterization was conducted in a spherical aberration-corrected TEM (Titan ChemiSTEM, FEI) at 200 kV. The quasi-static uniaxial tensile tests were carried out using an MTS Landmark servo hydraulic testing machine equipped with a remodeled environmental chamber at RT and liquid nitrogen temperature (LNT) at a strain rate of 5×10^{-4} s^{-1}. An extensometer was directly attached to the gauge section of straining samples to measure the strain during the tensile deformation. The electron backscatter diffraction (EBSD) sample was cut from the gauge section at a strain of 65%. The EBSD orientation maps were taken in a FEI Quanta 650 field emission gun scanning electron microscope equipped with EBSD system at a working distance of 15 mm at 20 kV. A beam step of 200 nm was set to obtain sufficient resolution in a relatively large analyzed area within reasonable acquisition time. Because some of the twins are quite thin, we also combined TEM observations in calculating the volume fraction of twins.

3. Results

3.1. Planar slip along twin boundaries

The formation of DT was observed at the early stage of plastic deformation as shown in Movie S1 and Fig. 1a. The propagation and thickening of DT occurred by the glide of massive partial dislocations with Burgers vector 1/6<112> on adjacent planes, similar to the previous observations [23,24]. When the twins formed, TBs acted as strong barriers to dislocation motion, impeding dislocation from passing through, and leading to dislocation pile up (marked by the blue arrow in Fig. 1). As the formation of deformation twins, the mean free path of dislocation slip was shortened, resulting in dynamic Hall–Petch strengthening effect.

Supplementary video related to this article can be found at https://doi.org/10.1016/j.mtnano.2018.11.004.

However, the formation of mechanical twinning was less observed during the further straining. The density of twins within the grain was low. It is then considered that the strain accommodated by twinning deformation was limited. Interestingly as shown in Fig. 1a and b (Movie S1), intensive planar slips of dislocations along the TBs which would contribute to plastic strain were found. This is similar to the previously reported easy glide of dislocations on or near TBs in high entropy alloys [25]. The glide of those dislocations did not lead to the thickening of twin because they were paired partial dislocations and their glide would not change the ABCABC sequence. In addition, dislocation slip along the TBs was faster than that in the matrix or within twins because there was almost no image force on dislocations when their Burgers vector paralleled to TBs [26,27]. The intersection of twins further constructed a channel for easy glide of dislocations where the dislocations cross slip from one TB to another, resulting in three-dimensional homogeneous deformation. That is, in addition to the contribution of mechanical twinning to plastic deformation, TB-assisted dislocation slip was an important contributor to plastic deformation.

3.2. Massive cross-slips and significant dislocation interactions

Dislocation slip is the dominant deformation mechanism at low strain stage for most of the fcc alloys with relatively low SFE. Fig. 2 shows the typical dislocation behaviors during the early stage of plastic deformation of the TWIP steel at RT. The planar slip of partial dislocations bounded with stacking faults was observed abundantly, as shown in Fig. 2a and Movie S2. In this material, the extension of dislocation and slip planarity are expected because the separation of a perfect dislocation into two partial dislocations linked with a stacking fault in between is energetically favorable due to low SFE. The width of stacking faults is changing dynamically during the glide of partial dislocations. As the glide of leading partial is impeded by local obstacles, the width of stacking fault decreases, whereas the slow motion of trailing partial would consequently increase the width of stacking fault. In general, the dissociation is thought to facilitate planar slip and prevent cross-slip; even the width of stacking fault is narrow [2]. These

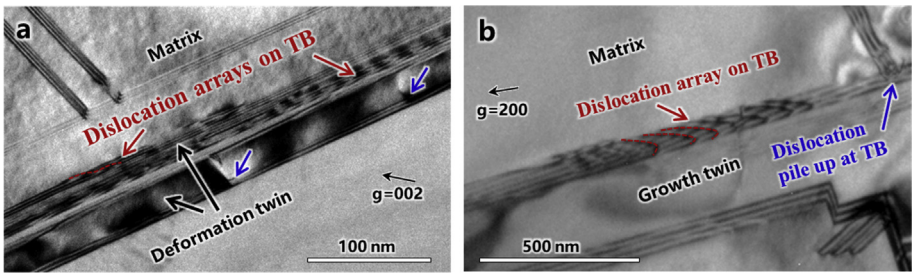

Fig. 1. Twin boundaries (TBs) taking effect on plastic deformation as dislocation slipping pathways and obstacles. **(a)** Dislocation array moving on the deformation twin boundary. **(b)** Dislocation pile up at growth twin boundary and dislocation arrays on twin boundary.

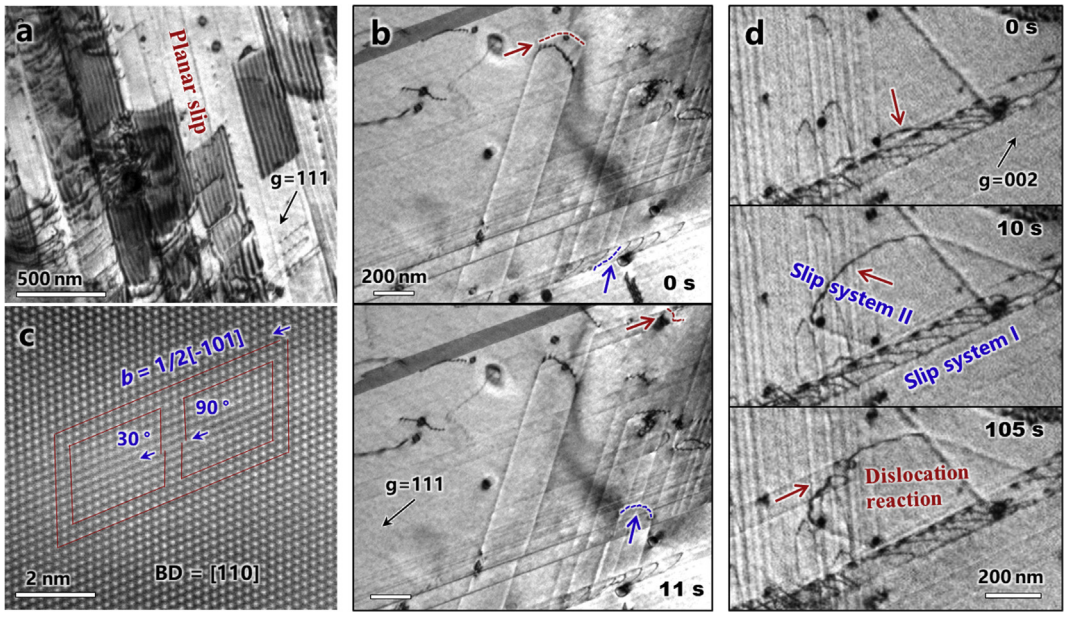

Fig. 2. Dislocation activities and dislocation atomic structure in the twinning-induced plasticity steel at room temperature. **(a)** Planar slip of partial dislocations. **(b)** Cross-slip of dislocations (marked by red and blue dotted lines). **(c)** Atomic structure of the cross-slip dislocation and the full Burgers vector is determined to be 1/2[−101]; beam direction (BD) = [110]. **(d)** Dislocation reaction of cross-slip dislocation and dislocation in another primary slip plane.

dislocation behaviors are considered less to work hardening. Besides, the extension would also affect the climb of dislocations [28].

Supplementary video related to this article can be found at https://doi.org/10.1016/j.mtnano.2018.11.004.

It is thought that the extension of dislocation would hinder cross-slip because the latter one requires partial dislocations recombination or dislocation reaction [29,30]. However, massive cross-slips of dislocations were repeatedly captured (Fig. 2b and Movie S3) in the TWIP steel during our *in situ* TEM straining tests at RT. The cross-slipped dislocations were marked by red and blue dotted lines and arrows in Fig. 2b. Cross-slip events occurred randomly along the planar slip but with high frequency. Although the cross-slip phenomenon in TWIP steels was previously mentioned by Choi et al. [22] in micro-pillar compression test, our results are different in terms of the intensity of cross-slip, stress level, and *in situ* observation.

Supplementary video related to this article can be found at https://doi.org/10.1016/j.mtnano.2018.11.004.

Fig. 2c demonstrates the atomic structure of the cross-slip dislocations, viewing along [110] direction. The atomic scale core structure of an extended dislocation on the primary plane was clearly resolved. It contains a stacking fault of about 4 nm in width. And the Burgers circle analysis in red determined that the full Burgers vector of the extended dislocation is $\boldsymbol{b} = 1/2[-101]$, indicating that the dislocations in primary slip plane were oriented in a mixed configuration. Whereas only the screw component could cross slip, the edge segments left in the primary slip band acting as obstacles for primary dislocation motion, which would further promote cross-slip process. As previously reported, cross-slip could stabilize three-dimension dislocation configuration by forming Lomer–Cottrell locks, which acts as a critical hardening element [30]. Regrettably, low SFE makes the cross-slip much difficult.

By promoting cross slip, dislocation–dislocation interaction was enhanced. Sequence bright field images in Fig. 2d and Movie S4 show the dynamic cross-slip of a dislocation and the further interaction of the cross-slipped dislocation with a dislocation from the original planar slip system. The two dislocations were broken into two segments, respectively; the segments of dislocation in slip system II combined with the segments of dislocation of slip system I. As a consequence, the glissile dislocations were pinned. According to previous reports, the pinned dislocations could serve as dislocation multiplication sources [31] or could be a nucleate site for twinning [23,32]. Nevertheless, multislips and DT can be enhanced. Thus, it is thought that massive cross-slips of dislocations play an important role in facilitating dislocation–dislocation interaction and DT, which doubtless promote the formation of complex, tangled dislocation network for hardening and three dimensional homogeneous plastic deformation.

Supplementary video related to this article can be found at https://doi.org/10.1016/j.mtnano.2018.11.004.

3.3. Holistic perspective of twinning in bulk sample

To quantitatively analyze the macroscopic contribution of twinning and dislocation plasticity to deformation, we further performed EBSD analysis combining with TEM characterization to count the proportion of twins in the deformed samples as shown in Fig. 3. A modified Fullman equation was used to determine the volume fraction of twins in twinned grains [33],

$$f = \frac{2t}{l + 2t}$$

where f is the volume fraction of twins, l is the mean distance between two twins, and t is the mean thickness of twin lamella.

EBSD maps were displayed as inverse pole figure maps and band contrast maps in the vertical direction of the tensile axis as shown in Fig. 3a and b. Inverse pole figure map presents the orientation of grains and shows the orientation of twins and matrix, as indicated by red lines in Fig. 3b. To achieve better resolution, the finer mechanical twins were identified from the band contrast maps in which the dark dots represent the overlap of two Kikuchi patterns of matrix and twin. Thus, the dark plate-like products depict the mechanical twins.

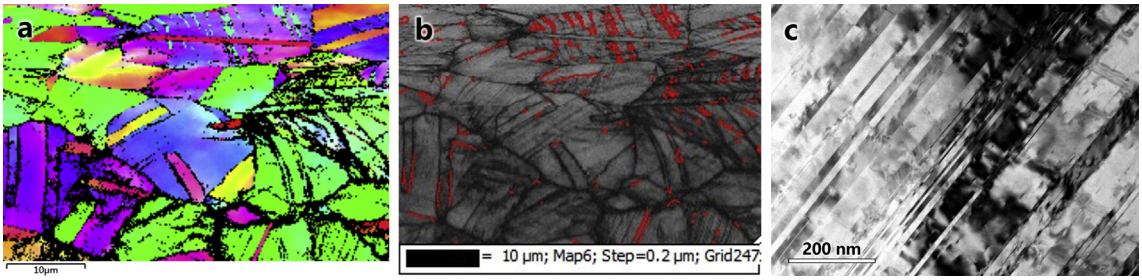

Fig. 3. Distribution of twins in twinning-induced plasticity (TWIP) steel deformed by macrotensile tests. **(a)** Inverse pole figure and **(b)** band contrast electron backscatter diffraction maps of the TWIP steel at a strain of 0.65. The red lines in **(b)** indicate the twin boundaries. **(c)** Bright field image showing the spacing and thickness of mechanical twins.

The entire volume fraction of twins was determined to be the volume percentage of twins in twinned grain multiplied by the ratio of twinned grains. From EBSD and TEM characterizations, the volume fraction of deformation twins in average in the entire sample was determined to be about 8%, which was in good agreement with previous theoretical and experimental studies [13]. It indicates that the contribution of DT to plasticity and hardening was rather limited. In contrast to what previously reported in literatures, TBs were also found to facilitate dislocation activities by providing pathway for dislocation glide.

3.4. Dislocation activity–induced nanocrystallization

As load increased, high density of dislocation networks formed in the matrix. The mobility of dislocation relatively decreased. In contrast, as crack initiated at the later stage of plastic deformation, dislocation motions at the crack tip were still rapid due to the stress concentration. Interestingly, it was found that the severe dislocation activities resulted in grain refinement. One single grain was gradually divided into nanograins at the crack tip. The upper-right insets in Fig. 4a and c are diffraction patterns taken at the crack tip region before and after *in situ* TEM straining, which clearly illustrated single crystal feature at the initial state and polycrystalline feature after severe plastic deformation, respectively. The high resolution TEM sequence images in Fig. 4 show the dynamic process of the transformation from a single crystal to multiple nano-sized grains with a size of about 10 nm. During grain refinement, only partial dislocation movements were observed as shown in Fig. 4b.

Because TEM observation only provides two-dimensional structure information, we still need more information to fully reconstruct the dynamic transformation process in real space. However, it was confirmed that only dislocation activities were involved during transformation. We believed that the intense dislocation movements caused by the extremely high stress at the crack tip were main carriers of plastic deformation there and the activation of multiple partial dislocation glides led to nanocrystallization in certain ways. Thus, besides the mechanism of grain refinement by DT [34], highly intense partial dislocation movements should also be a mechanism of nanocrystallization in TWIP steel materials. Deformation-induced grain refinement could simultaneously enhance mechanical properties at the later stage of homogeneous plastic deformation [35]. In this work, it was observed that crack propagated along the nanograins after nanocrystallization, resulting in a nanoscale zigzag pattern of the crack propagation path (Movie S5), which may significantly enhance the toughness of material.

Supplementary video related to this article can be found at https://doi.org/10.1016/j.mtnano.2018.11.004.

3.5. Temperature effect on dislocation activity

To investigate the temperature dependence of dislocation activity in TWIP steels, we studied the dislocation activity *in situ* as well as macroscopic uniaxial tensile properties ex situ at RT and cryogenic temperature. The engineering stress–strain curves obtained from tensile experiments at RT and LNT were both plotted in Fig. 5a. As temperature decreased from RT to LNT, the ultimate tensile strength increased dramatically, from ~800 MPa to ~1400 MPa, whereas the elongation at break increased slightly, from ~0.65 to ~0.7.

It demonstrates that the TWIP steel exhibited much higher strength and relatively larger elongation at cryogenic temperature. This is similar to some recent observations in high entropy alloys [9] but is different to many traditional alloys in which ductility decreases as temperature reduces. Theoretically, dislocation activities would be suppressed at cryogenic temperature, because the Peierls–Nabarro barrier increases and SFE decreases as

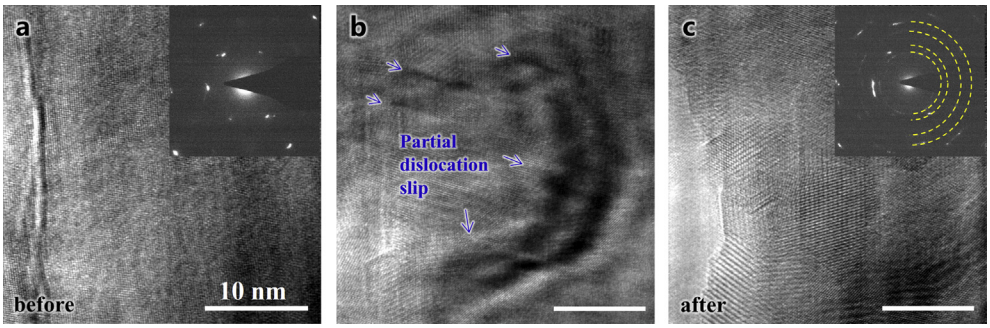

Fig. 4. Single crystal transformed into nanocrystal at the crack tip. **(a)**, **(c)** High-resolution TEM images of crystal lattice before and after deformation. The corresponding diffraction patterns are shown at the upper right. The initial beam direction was [110] and final one turned into polycrystal ring. **(b)** Partial dislocations slipping during nanocrystallization process. Multiple dislocation slips are indicated by blue arrows. TEM, transmission electron microscope.

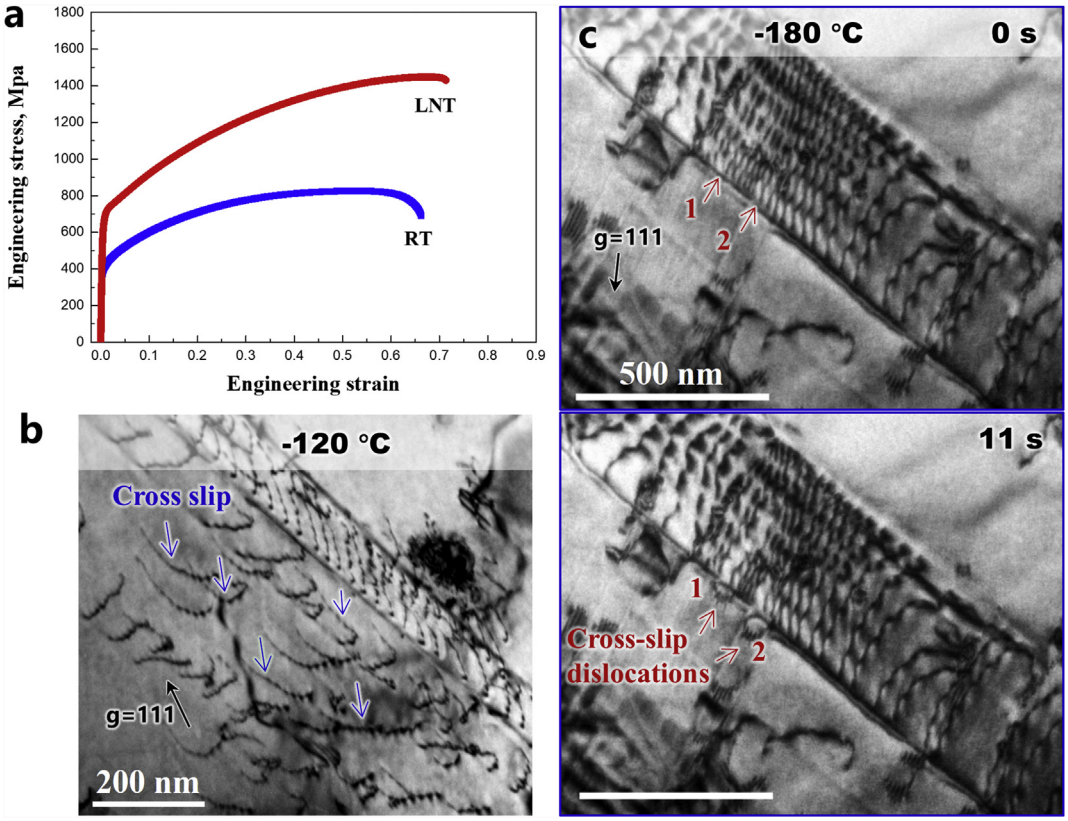

Fig. 5. Temperature dependence of mechanical property and dislocation activity. **(a)** The temperature dependence of tension stress–strain curve, in which the samples were deformed at liquid nitrogen temperature (LNT) and room temperature (RT). **(b)** Bright field image showing detailed cross-slip of dislocation at −120 °C. **(c)** Bright field image sequences showing dynamic cross-slip of dislocations at −180 °C.

temperature reduces. The better cryogenic ductility is highly related to the deformation-induced nano-twinning in high entropy alloys [9]. However, we found that glissile dislocations maintained their activities which were comparable with those at RT in the TWIP steel. Besides the ordinary dislocation slip, massive cross-slips were observed at low temperature as well, which is opposite to our traditional understanding that cross-slip of dislocations as a thermally activated process generally happens at elevated temperature. Fig. 5b and c (Movie S6 and Movie S7) show the cross-slip process of screw dislocations at −120 °C and −180 °C, respectively. The blue arrows in Fig. 5b indicated the cross-slip directions at −120 °C, and the red arrows in Fig. 5c pointed out the cross-slip dislocations from a dense dislocation array in the primary slip band at −180 °C.

Supplementary video related to this article can be found at https://doi.org/10.1016/j.mtnano.2018.11.004.

4. Discussion

The above observations demonstrated that dislocation activities played very important roles in accommodating plastic strain. In particular, the appearance of massive cross-slips during the plastic deformation of TWIP steels was thought to be unlikely before. The cross-slip usually occurs easily in a metal of high SFE. A screw dislocation leaves its glide plane and propagates to a conjugative one. Such a process can decrease internal stress fields, for example, by dislocation pile-ups. From this, cross-slip plays a key role macroscopically in plasticity to reduce the strain hardening rate during the stage-III hardening [36]. In contrast, low SFE makes the cross-slip difficult because of splitting of a dislocation. A gliding perfect dislocation consists of two dissociated partials separated by a stacking fault. The lower the SFE, the wider the stacking fault will be. This large separation between two partials inhibits cross-slip and makes dislocations organize themselves into a more uniform dislocation structure, e.g. planar arrays as shown in Fig. 2a. Once cross slipping, the leading partial first changes its glide plane to create a stair rod dislocation [37], with which the trailing partial reacts thereby also to change its glide plane. Such a process of cross-slip falls under a class of mechanisms commonly referred to as the Fleischer mechanism [38]. The cross-slip helps out to enhance plasticity and strain hardening in several aspects. First, the stacking fault between partials must be eliminated for the dislocation to cross slip. A high applied stress is, thus, needed to activate the slip of trailing partials with straining. Second, the cross-slip increases the possibility for dislocation–dislocation interactions, via the annihilation of tangled dislocations formed at an early stage of straining. The basic dislocation substructures in stage-III hardening are produced by cross-slip. The onset of stage-III work hardening is attributed to cross-slip in a metal [39–41]. It is observed that the stage-III work-hardening is closely analogous between fcc and bcc metals. This is due to the easy cross-slip of screw dislocations in both cases. Finally, the cross-slip increases the probability of dislocation intersections in varying slip planes and therefore, facilitates the generation of varying jogs, junctions, and locks [41], as a substantial mechanism for strain hardening.

Although future work is required to systematically analyze the density of jogs and locks created by cross-slip and their contribution to work hardening, for the first time, our *in situ* tensile observation exhibits the experimental evidence of massive cross-slips during the tensile deformation of a TWIP steel. This result

sheds light on a new perspective on understanding the effect of DT and dislocation activities in TWIP steels to help out both high tensile strength and high ductility.

Competing financial interest statement

The authors declare no competing financial interests.

Data availability

The raw/processed data required to reproduce these findings cannot be shared at this time as the data also forms part of an ongoing study.

Acknowledgments

This work was supported by grants from the Chinese 1000-Youth-Talent Plan (for Q.Y.), 111 project under Grant No. B16042 (for Q. Y.), National Natural Science Foundation of China (51671168) and the State Key Program for Basic Research in China under grant no. 2015CB65930. XiaoLei Wu was supported by the National Key R&D Program of China 2017YFA0204402, the National Natural Science Foundation of China (Grant Nos. 11572328 and 11790293), and the Strategic Priority Research Program of the Chinese Academy of Sciences (Grant No. XDB22040503).

References

[1] O. Grässel, L. Krüger, G. Frommeyer, L.W. Meyer, High strength Fe–Mn–(Al, Si) TRIP/TWIP steels development-properties-application, Int. J. Plast. 16 (2000) 1391–1409. https://doi.org/10.1016/S0749-6419(00)00015-2.
[2] O. Bouaziz, S. Allain, C.P. Scott, P. Cugy, D. Barbier, High manganese austenitic twinning induced plasticity steels: a review of the microstructure properties relationships, Curr. Opin. Solid State Mater. Sci. 15 (2011) 141–168. https://doi.org/10.1016/j.cossms.2011.04.002.
[3] K. Renard, P.J. Jacques, On the relationship between work hardening and twinning rate in TWIP steels, Mater. Sci. Eng. A 542 (2012) 8–14. https://doi.org/10.1016/j.msea.2012.01.123.
[4] J.K. Kim, M.H. Kwon, B.C. De Cooman, On the deformation twinning mechanisms in twinning-induced plasticity steel, Acta Mater. 141 (2017) 444–455. https://doi.org/10.1016/j.actamat.2017.09.043.
[5] L. Remy, Kinetics of f.c.c. deformation twinning and its relationship to stress-strain behaviour, Acta Metall. 26 (1978) 443–451. https://doi.org/10.1016/0001-6160(78)90170-0.
[6] H. Beladi, I.B. Timokhina, Y. Estrin, J. Kim, B.C. De Cooman, S.K. Kim, Orientation dependence of twinning and strain hardening behaviour of a high manganese twinning induced plasticity steel with polycrystalline structure, Acta Mater. 59 (2011) 7787–7799. https://doi.org/10.1016/j.actamat.2011.08.031.
[7] I.C. Jung, B.C. De Cooman, Temperature dependence of the flow stress of Fe-18Mn-0.6C-xA1 twinning-induced plasticity steel, Acta Mater. 61 (2013) 6724–6735. https://doi.org/10.1016/j.actamat.2013.07.042.
[8] G. Dini, R. Ueji, A. Najafizadeh, S.M. Monir-Vaghefi, Flow stress analysis of TWIP steel via the XRD measurement of dislocation density, Mater. Sci. Eng. A 527 (2010) 2759–2763. https://doi.org/10.1016/j.msea.2010.01.033.
[9] B. Gludovatz, A. Hohenwarter, D. Catoor, E.H. Chang, E.P. George, R.O. Ritchie, A fracture-resistant high-entropy alloy for cryogenic applications, Science 345 (2014) 1153–1158. https://doi.org/10.1126/science.1254581.
[10] B. Gludovatz, A. Hohenwarter, K.V.S. Thurston, H. Bei, Z. Wu, E.P. George, R.O. Ritchie, Exceptional damage-tolerance of a medium-entropy alloy CrCoNi at cryogenic temperatures, Nat. Commun. 7 (2016). https://doi.org/10.1038/ncomms10602.
[11] Z. Zhang, M.M. Mao, J. Wang, B. Gludovatz, Z. Zhang, S.X. Mao, E.P. George, Q. Yu, R.O. Ritchie, Nanoscale origins of the damage tolerance of the high-entropy alloy CrMnFeCoNi, Nat. Commun. 6 (2015). https://doi.org/10.1038/ncomms10143.
[12] F. Otto, A. Dlouhý, C. Somsen, H. Bei, G. Eggeler, E.P. George, The influences of temperature and microstructure on the tensile properties of a CoCrFeMnNi high-entropy alloy, Acta Mater. 61 (2013) 5743–5755. https://doi.org/10.1016/j.actamat.2013.06.018.
[13] B.C. De Cooman, Y. Estrin, S.K. Kim, Twinning-induced plasticity (TWIP) steels, Acta Mater. 142 (2018) 283–362. https://doi.org/10.1016/j.actamat.2017.06.046.
[14] H.K. Yang, V. Doquet, Z.F. Zhang, Micro-scale measurements of plastic strain field, and local contributions of slip and twinning in TWIP steels during in situ tensile tests, Mater. Sci. Eng. A 672 (2016) 7–14. https://doi.org/10.1016/j.msea.2016.06.064.
[15] O. Bouaziz, S. Allain, C. Scott, Effect of grain and twin boundaries on the hardening mechanisms of twinning-induced plasticity steels, Scripta Mater. 58 (2008) 484–487. https://doi.org/10.1016/j.scriptamat.2007.10.050.
[16] N. Li, J. Wang, A. Misra, X. Zhang, J.Y. Huang, J.P. Hirth, Twinning dislocation multiplication at a coherent twin boundary, Acta Mater. 59 (2011) 5989–5996. https://doi.org/10.1016/j.actamat.2011.06.007.
[17] K. Lu, L. Lu, S. Suresh, Strengthening materials by engineering coherent internal boundaries at the nanoscale, Science 324 (2009) 349–352. https://doi.org/10.1126/science.1159610.
[18] X.L. Wu, Y.T. Zhu, Y.G. Wei, Q. Wei, Strong strain hardening in nanocrystalline nickel, Phys. Rev. Lett. 103 (2009) 205504. https://doi.org/10.1103/PhysRevLett.103.205504.
[19] L. Lu, Y. Shen, X. Chen, L. Qian, K. Lu, Ultrahigh strength and high electrical conductivity in copper, Science 304 (2004) 422–426. https://doi.org/10.1126/science.1092905.
[20] I. Gutierrez-Urrutia, D. Raabe, Dislocation and twin substructure evolution during strain hardening of an Fe–22 wt.% Mn–0.6 wt.% C TWIP steel observed by electron channeling contrast imaging, Acta Mater. 59 (2011) 6449–6462. https://doi.org/10.1016/j.actamat.2011.07.009.
[21] Z.Y. Liang, Y.Z. Li, M.X. Huang, The respective hardening contributions of dislocations and twins to the flow stress of a twinning-induced plasticity steel, Scripta Mater. 112 (2016) 28–31. https://doi.org/10.1016/j.scriptamat.2015.09.003.
[22] W.S. Choi, B.C. De Cooman, S. Sandlöbes, D. Raabe, Size and orientation effects in partial dislocation-mediated deformation of twinning-induced plasticity steel micro-pillars, Acta Mater. 98 (2015) 391–404. https://doi.org/10.1016/j.actamat.2015.06.065.
[23] G. Casillas, A.A. Gazder, E.V. Pereloma, A.A. Saleh, Evidencing extrinsic stacking faults in twinning-induced plasticity steel, Mater. Char. 123 (2017) 275–281. https://doi.org/10.1016/j.matchar.2016.11.039.
[24] J.W. Christian, S. Mahajan, Deformation twinning, Prog. Mater. Sci. 39 (1995) 1–157. https://doi.org/10.1016/0079-6425(94)00007-7.
[25] Z. Zhang, H. Sheng, Z. Wang, B. Gludovatz, Z. Zhang, E.P. George, Q. Yu, S.X. Mao, R.O. Ritchie, Dislocation mechanisms and 3D twin architectures generate exceptional strength-ductility-toughness combination in CrCoNi medium-entropy alloy, Nat. Commun. 8 (2017) 14390. https://doi.org/10.1038/ncomms14390.
[26] L. Priester, O. Khalfallah, Image force on a lattice dislocation due to a grain boundary in anisotropic f.c.c. materials, Philos. Mag. A 69 (1994) 471–484. https://doi.org/10.1080/01418619408242225.
[27] Y. Koizumi, S. Suzuki, K. Yamanaka, B.-S. Lee, K. Sato, Y. Li, S. Kurosu, H. Matsumoto, A. Chiba, Strain-induced martensitic transformation near twin boundaries in a biomedical Co–Cr–Mo alloy with negative stacking fault energy, Acta Mater. 61 (2013) 1648–1661. https://doi.org/10.1016/j.actamat.2012.11.041.
[28] J.P. Hirth, J. Lothe, Theory of Dislocations, second ed., McGraw-Hill, New York, 1986.
[29] Y. Deng, C.C. Tasan, K.G. Pradeep, H. Springer, A. Kostka, D. Raabe, Design of a twinning-induced plasticity high entropy alloy, Acta Mater. 94 (2015) 124–133. https://doi.org/10.1016/j.actamat.2015.04.014.
[30] W. Püschl, Models for dislocation cross-slip in close-packed crystal structures: a critical review, Prog. Mater. Sci. 47 (2002) 415–461. https://doi.org/10.1016/S0079-6425(01)00003-2.
[31] J.S. Koehler, The nature of work-hardening, Phys. Rev. 86 (1952) 52–59.
[32] N. Naeita, J. Takamura, Deformation twinning in silver-and copper-alloy crystals, Philos. Mag. A J. Theor. Exp. Appl. Phys. 29 (1974) 1001–1028. https://doi.org/10.1080/14786437408226586.
[33] A. Soulami, K.S. Choi, Y.F. Shen, W.N. Liu, X. Sun, M.A. Khaleel, On deformation twinning in a 17.5% Mn–TWIP steel: a physically based phenomenological model, Mater. Sci. Eng. A 528 (2011) 1402–1408. https://doi.org/10.1016/j.msea.2010.10.031.
[34] K. Lu, J. Lu, Nanostructured surface layer on metallic materials induced by surface mechanical attrition treatment, Mater. Sci. Eng. A 375 (2004) 38–45. https://doi.org/10.1016/j.msea.2003.10.261.
[35] D.C.C. Magalhães, A.M. Kliauga, M. Ferrante, V.L. Sordi, Plastic deformation of FCC alloys at cryogenic temperature: the effect of stacking-fault energy on microstructure and tensile behaviour, J. Mater. Sci. 52 (2017) 7466–7478. https://doi.org/10.1007/s10853-017-0979-8.
[36] P.J. Jackson, The role of cross-slip in the plastic deformation of crystals, Mater. Sci. Eng. 57 (1983) 39–47. https://doi.org/10.1016/0025-5416(83)90025-3.
[37] M.J. Marcinkowski, R.J. Taunt, K. Sadananda, Effect of stacking fault energy on the mutual cross slip of unlike dislocations—II stair rod mode, Acta Metall. 22 (1974) 1415–1421. https://doi.org/10.1016/0001-6160(74)90042-X.
[38] R.L. Fleischer, Cross slip of extended dislocations, Acta Metall. 7 (1959) 134–135. https://doi.org/10.1016/0001-6160(59)90122-1.
[39] Z.Q. Wang, I.J. Beyerlein, R. LeSar, The importance of cross-slip in high-rate deformation, Model. Simulat. Mater. Sci. Eng. 15 (2007) 675. https://doi.org/10.1088/0965-0393/15/6/006.
[40] G. Saada, Cross-slip and work hardening of f.c.c. crystals, Mater. Sci. Eng. A 137 (1991) 177–183. https://doi.org/10.1016/0921-5093(91)90333-I.
[41] B. Šesták, A. Seeger, The relationship between the work-hardening of B.C.C. And F.C.C. Metals, Phys. Status Solidi (b) 43 (1971) 433–444. https://doi.org/10.1002/pssb.2220430146.